Toxicology in Vitro 96 (2024) 105770

Contents lists available at ScienceDirect

Toxicology in Vitro

journal homepage: www.elsevier.com/locate/toxinvit

Screening for endocrine disrupting chemicals inhibiting monocarboxylate 8 (MCT8) transporter facilitated thyroid hormone transport using a modified nonradioactive assay

Fabian Wagenaars [a], Peter Cenijn [a], Martin Scholze [b], Caroline Frädrich [c], Kostja Renko [d], Josef Köhrle [c], Timo Hamers [a,*]

[a] Amsterdam Institute for Life and Environment (A-Life), Vrije Universiteit Amsterdam (VU), De Boelelaan 1085, 1081, HV, Amsterdam, the Netherlands
[b] Brunel University London, Centre for Pollution Research and Policy, College of Health, Medicine and Life Sciences, Kingston Lane, Uxbridge UB8 3PH, UK
[c] Charité – Universitätsmedizin Berlin, Corporate member of Freie Universität Berlin and Humboldt Universität zu Berlin Institut für Experimentelle Endokrinologie, Hessische Strasse 3-4, 10115 Berlin, Germany
[d] German Centre for the Protection of Laboratory Animals (Bf3R), Bundesinstitut für Risikobewertung (BfR), Berlin, Germany

ARTICLE INFO

Editor: Dr. J Davila

Keywords:
Endocrine disrupting chemicals
In vitro assays
Monocarboxylate 8 transporter
Sandell-Kolthoff reaction
Thyroid hormones

ABSTRACT

Early neurodevelopmental processes are strictly dependent on spatial and temporally modulated of thyroid hormone (TH) availability and action. Thyroid hormone transmembrane transporters (THTMT) are critical for regulating the local concentrations of TH, namely thyroxine (T4) and 3,5,3′-tri-iodothyronine (T3), in the brain. Monocarboxylate transporter 8 (MCT8) is one of the most prominent THTMT. Genetically induced deficiencies in expression, function or localization of MCT8 are associated with irreversible and severe neurodevelopmental adversities. Due to the importance of MCT8 in brain development, studies addressing chemical interferences of MCT8 facilitated T3 uptake are a crucial step to identify TH system disrupting chemicals with this specific mode of action. Recently a non-radioactive *in vitro* assay has been developed to rapidly screen for endocrine disrupting chemicals (EDCs) acting upon MCT8 mediated transport. This study explored the use of an UV-light digestion step as an alternative for the original ammonium persulfate (APS) digestion step. The non-radioactive TH uptake assay, with the incorporated UV-light digestion step of TH, was then used to screen a set of 31 reference chemicals and environmentally relevant substances to detect inhibition of MCT8-depending T3 uptake. This alternative assay identified three novel MCT8 inhibitors: methylmercury, bisphenol-AF and bisphenol-Z and confirmed previously known MCT8 inhibitors.

1. Introduction

Iodothyronines are a broad set of (pro-)hormones and metabolites. The most prominent ones are the pro-hormone thyroxine (T4), exclusively produced by the thyroid gland, and the biologically active 3,5,3′-tri-iodothyronine (T3), usually summarized as thyroid hormones (TH). TH are essential in regulating development and function of many organs, but are particularly important during a critical period of

Abbreviations: 3–3'T2, 3–3'diodothyronine; AHDS, Allan-Herndon-Dudley syndrome; AMI, amitrole; APS, ammonium persulfate; BBB, blood-brain-barrier; BCSFB, blood-cerebral-spinal-fluid barrier; BMC, benchmark concentration; BMR, benchmark response level; BP-2, 2,2′,4,4′-tetrahydroxybenzophenone; BPA, bisphenol-A; BPAF, bisphenol-AF; BPF, bisphenol-F; BPS, bisphenol-S; BPZ, bisphenol-Z; BSP, bromosulfopthalein; CYN, cyanamide; DAIZ, daidzein; DASA, dasatinib; DBP, di-(n)-butylphthlate; DIC, diclofenac; DIO, deiodinase; DMI, desipramine; DMSO, dimethylsulfoxide; EDC, endocrine disrupting chemicals; EMO, emodin; IC, inhibitory concentration; ICG, indocyanine green; IMI, imidacloprid; LDH, lactate dehydrogenase; MBI, 2-mercaptobenzimidazole; MCT8, monocarboxylate transporter 8; MDCK, Madin Darby canine kidney; MeHg, methyl mercury; NADH, nicotinamide adenine dinucleotide; NaOH, sodium hydroxide; OATP1C1, organic anion transporter 1C1; PBS, phosphate-buffered saline; PCP, pentrachlorophenol; PFOA, perfluorooctanoic acid; PFOS, perfluorooctancesulfonic acid; PHL, phloretin; PRB, probenecid; PTU, propylthiouracil; rT3, reverse T3; SK, Sandell-Kolthoff; SUNI, sunitinib; SY, silychristin; T3, 3,5,3′-tri-iodothyronine; T4, thyroxine; TBBPA, tetrabromobisphenol-A; TBP, 2,4,6-tribromophenol; TBT, tributyltin; TH, thyroid hormone; THS, thyroid hormone system; THTMT, thyroid hormone transmembrane transporter; VRP, verapamil; WT, wildtype; XN, xanthohumol.

* Corresponding author at: De Boelelaan 1085, 1081, HV, Amsterdam, the Netherlands.
E-mail address: timo.hamers@vu.nl (T. Hamers).

https://doi.org/10.1016/j.tiv.2023.105770
Received 28 July 2023; Received in revised form 14 December 2023; Accepted 22 December 2023
Available online 25 December 2023

neurodevelopment. TH deficiency and excess are associated with severe neurological developmental problems resulting in irreversible adverse effects such as impaired cochlear hearing, mental retardation and loss of IQ (Andersen and Andersen, 2021; Zoeller et al., 2002). TH availability therefore is highly regulated through several systemic and local control mechanisms within the entire thyroid hormone system (THS). Circulating concentrations of TH are kept within a small individual range by regulation through negative feedback loops in the hypothalamus-pituitary-thyroid (HPT) axis (Gilbert et al., 2012), while intracellular concentrations are maintained by several local control mechanisms, including TH transmembrane transporters (THTMTs), intracellular deiodinases (DIOs) and TH metabolizing enzymes (Köhrle and Frädrich, 2021).

In early development until the 2nd trimester of pregnancy, the fetus is completely dependent on a maternal supply of TH, which in order to reach the fetal developing brain need to cross several physiological barriers, namely the placenta, blood-brain-barrier (BBB) and/−or the blood-cerebral-spinal-fluid barrier (BCSFB). TH transport across these physiological barriers is facilitated by THTMT, regulating bidirectional transport of charged TH from the systemic blood circulation into the cells as well as the transport across the barrier cells into the local blood circulation of the fetus (placenta) or the fetal brain (BBB/BCSFB). Among these THTMT, monocarboxylate 8 (MCT8) is one of the most crucial transporters known so far. MCT8 has a very narrow substrate spectrum and high specificity towards TH, transporting in order of preference T3 > T4 > reverse T3 (rT3) > 3–3'diodothyronine (3–3'T2) in overexpressing cell models (Friesema et al., 2006). MCT8 is also highly expressed in cerebral micro-vessels and -neurons, in choroid plexus epithelial cells, (Roberts et al., 2008), and in placental syncytiotrophoblast and cytotrophoblast cells (Loubière et al., 2010). Current data provides evidence, that MCT8 plays a major role in the uptake of TH from the bloodstream into epithelial and endothelial cells of both the BCSFB and BBB, while also involved in the uptake of T3 in neurons from astrocytic end-feet (Landers and Richard, 2017). The role of MCT8 in the placenta is less clear, due the complex cellular composition and organization of the maternal-fetal placental unit as well as suspected functional redundancy due to the presence of other TH transporters (Chen et al., 2022a). The importance of MCT8 as a major transporter regulating transport in the brain is further elucidated by patient mutations found in the MCT8 encoding gene SLC16A2. These mutations, leading to MCT8-deficiency, are linked with a severe neurodevelopment disorder called the Allan-Herndon-Dudley syndrome (AHDS) in human patients (Schwartz et al., 2005). Interestingly, the severity of MCT8-deficient phenotypes was shown to depend on the residual T3 transport capacity of the respective mutant (Kinne et al., 2009, 2010). Furthermore, in patient derived iPSCs *in vitro* models MCT8 deficiency is directly linked to a decreased transport of T3 across the BBB, which subsequently leads to delayed neuronal maturation (Vatine et al., 2017). A detailed view on the current state of knowledge on MCT8 is given in respective reviews (Groeneweg et al., 2019), in which clear and strong evidence is presented that disruption of the normal functioning of MCT8 has devastating effects on brain development in human beings.

It is therefore hypothesized that endocrine disrupting chemicals (EDCs) interfering with MCT8 facilitated TH transport potentially affect early neurodevelopment when exposure takes place in a vulnerable time window. Several tyrosine kinase inhibitors, including sunitinib (SUNI), dasatinib (DASA), imatinib and bosutinib, have been identified to inhibit cellular uptake of T3 *via* MCT8 *in vitro* (Braun et al., 2012; Kinne et al., 2009). These chemicals are also clinically linked to hypothyroidism, although other mechanisms than MCT8 inhibition have also been proposed as an underlying cause (Illouz et al., 2014). Silychristin (SY), a flavonoid present in milk thistle, was also identified as a highly specific and potent MCT8 inhibitor (Johannes et al., 2016). MCT8 inhibition by chemical interference has been identified as a putative molecular initiating event in the thyroidal adverse outcome pathway network and (pre-)validation of a respective protocol was initiated in the framework of the NETVAL Thyroid study (Noyes et al., 2019; Zuang et al., 2020). Given the importance and impact of MCT8 on brain TH concentrations and the lack of data on chemical inhibition of MCT8, there is clear need to consolidate and optimize respective HTS testing strategies that can identify chemicals acting upon MCT8.

A promising non-radioactive TH uptake assay has been developed to test potential EDCs for T3 uptake inhibition *via* MCT8 in a 96-well format (Jayarama-Naidu et al., 2015). Based on the measurement of iodide after digestion of cellular TH accumulation, this assay can be readily used to test a potentially interfering compounds in a cheap, fast and easy method. This non-radioactive assay makes use of a Madin Darby canine kidney (MDCK) cell line overexpressing MCT8 that is incubated with T3 in the presence or absence of a test chemical. If the test chemical has an MCT8 inhibiting capacity, these cells show a lower T3 uptake in its presence than in its absence. Subsequently to oxidative digestion of the cells with ammomiun persulfate (APS), T3 uptake into the cells is indirectly quantified using a colorimetric redox reaction between cerium and arsenate also known as the Sandell-Kolthoff (SK) reaction (Renko et al., 2012; Sandell and Kolthoff, 1937). In the SK reaction, Ce^{4+} (yellow) is reduced to Ce^{3+} (colorless), while As^{3+} is oxidized to As^{5+}(Sandell and Kolthoff, 1937). The kinetics of this reaction depends on the amount of iodide, present in the applied samples and representing the amount of intracellular T3. Since MDCK cells lack deiodinase activity (Leonard, 1986) they cannot produce iodide from TH themselves and therefore, the rate of destaining in the SK reaction is completely attributable to iodide originating from intracellular TH. This method seems highly suitable to screen for potential MCT8 inhibitors, with good reproducibility, high specificity and selectivity and a corresponding method has already been used to identify potential MCT8 inhibitors, including indocyanine green (ICG), desipramine (DMI), bromosulfopthalein (BSP), phloretin (PHL) and bisphenol-A (BPA) (Dong and Wade, 2017). Given the wide structural diversity of MCT8 inhibiting chemicals, there is a need for screening methods to test other chemicals, including industrial pollutants found in food or the environment, for their MCT8 inhibiting potency.

A crucial step in this uptake assay is the digestion of TH in the cell lysate by ammonium persulfate (APS) at 90 °C to release iodide for catalyzing the SK reaction. A drawback of using APS based digestion within the SK reaction is the potential loss of elemental iodine when it is oxidized by air (Shelor and Dasgupta, 2011). For other acid-based digestions a mean loss of 20% iodine has been reported (Patzeltová, 1993). Therefore, it would be helpful to reduce or even prevent the loss of iodine in APS-based digestion methods (Ohashi et al., 2000; Pino et al., 1996) and accordingly develop alternative techniques.

In the present study we explored an alternative method of TH digestion by replacing the APS digestion with an UV-light digestion. UV-light irradiation has previously been used as an alternative digestion method in the analysis of urinary iodine content with a good correlation to acid digestion methods (Tsuda et al., 1995). We further applied the modified digestion method in the TH uptake assay to screen a set of seven positive and three negative reference chemicals tested for their capacity to inhibit T3 uptake by MCT8. In addition, 22 environmentally relevant chemicals were tested in the TH uptake assay in order to identify possible EDCs.

2. Materials and methods

2.1. Materials

ICG and SUNI were purchased from Cayman Chemical (Uden, The Netherlands), PHL and emodin (EMO) from Acros Organics (Landsmeer, the Netherlands), imidacloprid (IMI) was obtained from Fluka (Geel, Belgium), bisphenol-S (BPS) and bisphenol-Z (BPZ) from TRC Canada (Toronto, Canada), BSP from Alfa Aesar (Kandel, Germany). All other chemicals were obtained from Sigma Aldrich (Zwijndrecht, the Netherlands). All chemicals were dissolved in dimethylsulfoxide

(DMSO). On the day of the experiment 10-fold stocks of the chemicals were prepared in uptake buffer as such to reach a final vehicle concentration of 0.1% DMSO. Cell culture plates were purchased from Greiner Bio one (Alphen aan de Rijn, the Netherlands). All other plastics used during the experiments were purchased from Sarstedt (Etten-Leur, The Netherlands).

2.2. Cell culture

MDCK cells, stably transfected with human MCT8 (MDCK-MCT8) as previously described, were kindly provided by Dr. Ulrich Schweizer and Dr. Doreen Braun from the University of Bonn (Braun et al., 2012). Cells were cultured in DMEM:F12 (L-glutamine, 15 mM HEPES) (Gibco) supplemented with (1% penicillin+streptomycin) and 10% fetal calf serum (Gibco). Cell cultures were incubated at 37 °C with 5% CO_2 saturation until 80% confluency.

2.3. APS and UV-light digestion methods experiments

Twelve concentrations of both T3 and T4 (0, 0.025, 0.05, 0.1, 0.2, 0.4, 0.5, 0.6, 0.8, 1, 2 and 4 μM) were prepared in either 0.6 M APS or 0.1 M NaOH. For the APS method, 50 μL of T3 or T4 dissolved in 0.6 M APS were pipetted in a 96 wells plate and incubated for 60 min at 90 °C. Plates were cooled to RT and 10 μL of the TH solution was transferred to a new 96 wells plate containing 40 μL of MilliQ purified water per well. Iodide concentrations in the plate were then quantified as described below. For UV-light digestion, the twelve concentrations of both T3 and T4 dissolved in 0.1 M NaOH were 5 times diluted in 0.1 M NaOH in a 96 wells plate. Subsequently, corresponding concentrations of iodide, three times the concentration of T3 and four times the concentration of T4 (100% digestion), were prepared from an iodide standard in 0.1 M NaOH and pipetted into the 96 wells plate. The plates were then irradiated with UV-light (295 nm) for 90 min or indicated exposure times in a custom-built device, consisting of a closed aluminum container with 96 UV LEDs (Rayvio RVXR-295-SM) each aligned to an individual well with an 10 mW radiant output (supplementary fig. S1). Temperature in the closed container was maintained at room temperature by a built-in cooling block. The plates were cooled to RT and then quantified as described below.

2.4. TH uptake assay

MDCK-MCT8 or MDCK-wildtype (MDCK-WT) cells were seeded into a 96-well plate at a seeding density of $2x10^5$cells/100 μL medium/well and incubated for 72 h. TH uptake assay was performed as described by Jayarama-Naidu et al., 2015. Briefly, seeded cells were kept at 37 °C and washed once in 200 μL warm (37 °C) phosphate-buffered saline (PBS). 80 μL uptake buffer (125 mM NaCl, 10 mM HEPES, 5 mM KCl, 1.3 mM $CaCl_2$, 1.2 mM $MgCl_2$, pH adjusted to 7.4 and freshly added 5.6 mM D-glucose) was added to each well. Subsequently 10 μL of a 10-fold stock of test chemical or corresponding control (0.1% DMSO as vehicle control and 10 μM SY as positive control) was added. The uptake assay started with the addition 10 μL of T3 in uptake buffer (final concentration, f.c. 10 μM) to each well for 30 min incubation unless stated otherwise. After 30 min, buffer was collected from the cells into a new 96 wells plate and stored at −80 °C for LDH determination. Cells were immediately rinsed twice with ice-cold PBS supplemented with 0.1% bovine serum albumin and once with ice-cold deionized water. Cells were sequentially lysed in 50 μL 0.1 M NaOH. After 20 min of continuously shaking, cell lysates were further diluted in a new 96-well plate by adding 10 μL of lysates to 40 μL of 0.1 M NaOH. A calibration curve of T3 (0, 0.075, 0.1, 0.2, 0.3, 0.4, 0.5, 0.6, 0.7, 0.8, 1 and 2 μM) dissolved in 0.1 M NaOH was added in a similar dilution to the same 96-well plate. Cell lysates were then irradiated with UV-light as previously described.

2.5. Iodide quantification

To quantify the amount of iodide, 50 μL of acidic cerium solution (25 mM $(NH_4)_4Ce(SO4)_4$ and 0.5 M H_2SO_4) was added to each well, together with 50 μL of sodium arsenite solution (25 mM $NaAsO_2$, 0.5 M H_2SO_4 and 0.2 M NaCl). The decrease in yellow-colored Ce(IV) was measured spectrophotometrically (415 nm) every 10 s for 20 min (RT, Multiskan™ FC Microplate Photometer, Thermo Fisher Scientific). Absorption values over time were plotted in Graph Pad Prism 8 and the rate constants were derived using a first-order kinetic non-linear regression model. TH or iodide concentrations in samples were obtained by interpolating the rate constants in a linear regression fit of internal calibration curves of either T3 or potassium iodide, depending on the type of experiment. Recoveries were calculated as a percentage of expected iodide concentrations. For the TH uptake assay, derived concentrations were converted to total picomole. A flowchart for the quantification of iodide recoveries is given in supplementary fig. S2.

2.6. Chemical screening for MCT8 inhibition

A total of 31 chemicals (Table 1) were selected for screening in the TH uptake assay based on data available in literature, including four negative chemicals (XN, BP-2, TBBPA and DAIZ) and eight positive chemicals (ICG, SUNI, SY, DMI, BSP, DASA, PHL, BPA) to investigate the performance of the assay. A range-finding screening for all chemicals was performed at a single high concentration of either 100 μM or 10 μM depending on solubility. Chemicals that caused <80% cellular T3 uptake compared to the vehicle control (*i.e.* >20% inhibition) in the initial screen were subsequently tested in eight concentrations to obtain a full concentration response pattern. All experiments were repeated at least three times as individual experiments with three technical replicates per control or per test concentration.

2.7. Cytotoxicity assays

Cytotoxicity assays were performed to exclude that inhibited TH uptake in the assay was due to cell death or decreased cell viability. Resazurine assays, in which the conversion of resazurine to fluorescent resorufin by mitochondrial enzymes is measured, are commonly used to determine cell viability. Additionally, lactate dehydrogenase (LDH) leakage assays that quantify the amount of LDH released upon damage to the plasma membrane, are used to determine cell death.

Resazurine stocks (440 μM) were prepared in uptake buffer and kept at −80 °C. MCT8-MDCK cells were plated as described for the TH uptake assay. Cells were kept at 37 °C and washed once in 200 μL warm PBS (37 °C). Cells were then exposed to 100 μL uptake buffer, containing 70 μM resazurine, 10 μL of 10-fold of inhibitor or vehicle control and 10 μL of T3 (f.c. 10 μM). Fluorescence at 585 nm ($\lambda_{ex} = 550$ nm; $\lambda_{em} = 585$ nm) was measured at $t = 0$ and $t = 60$ min. Background signal at t = 0 was subtracted from the values at $t = 60$. All experiment were performed as three individual experiments with three technical replicates. Cell viability was determined as the ratio (expressed as a fraction) of the background corrected fluorescence values of cells exposed to the positive control, 4 mM Copper (II) sulfate, and cells exposed to the vehicle control. Concentrations were considered cytotoxic when viability was below 80% of vehicle control (IC20).

For the LDH leakage assay, the exposure medium collected from the TH uptake assay was thawed at room temperature. From each well 50 μL of the exposure medium was transferred into a new 96 wells plate. Additionally, 50 μL from cells exposed to lysis buffer was transferred into the new 96 wells plate as a positive control. Similarly, 50 μL from exposure medium without inhibitor or cells was used as a negative control. A reaction mix was prepared of 0.17 mg/mL reduced nicotinamide adenine dinucleotide (NADH) and 0.084 mg/mL sodium pyruvate dissolved in 100 mL 0.1 M potassium phosphate buffer (pH = 7.5). In each well 200 μL was added to the exposure medium and mixed

Table 1
Test chemicals and their inclusion criteria.

CAS	Chemical	Abbreviation	Reason for inclusion	Reference
486–66-8	daidzein	DAIZ	negative control	Johannes et al., 2016
119–61-9	2,2′,4,4′-tetrahydroxybenzophenone	BP-2	negative control	Johannes et al., 2016
6754-58-1	xanthohumol	XN	negative control	Johannes et al., 2016
79–94-7	tetrabromobisphenol-A	TBBPA	negative control	Dong and Wade, 2017
3599-32-4	indocyanine green	ICG	positive control	Dong and Wade, 2017
33,889–69-9	silychristin	SY	positive control	Johannes et al., 2016
341,031–54-7	sunitinib	SUNI	positive control	Braun et al., 2012; Dong and Wade, 2017
302,962–49-8	dasatinib	DASA	positive control	Braun et al., 2012; Dong and Wade, 2017
58–428-6	desipramine	DMI	positive control	Dong and Wade, 2017
71–67-0	bromosulfophthalein	BSP	positive control	Dong and Wade, 2017
60–82-2	phloretin	PHL	positive control	Dong and Wade, 2017
51–52-5	propylthiouracil	PTU	TPO inhibitor	Friedman et al., 2016
1763-23-1	perfluorooctanesulfonic acid	PFOS	NIS inhibitor	Buckalew et al., 2020
335–67-1	perfluorooctanoic acid	PFOA	TTR binding	Weiss et al., 2009
15,307–79-6	diclofenac	DIC	OATP1C1 inhibitor	Westholm et al., 2009
1461-22-9	tributyltin	TBT	TR transcription inhibitor	Sharan et al., 2014
138,261–41-3	imidacloprid	IMI	T3-antagonist	Xiang et al., 2017
87–86-5	pentachlorophenol	PCP	TTR binding	Ishihara et al., 2003; Hamers et al., 2006
84–74-2	di-(n)-butylphthlate	DBP	T3 uptake inhibitor	Shimada and Yamauchi, 2004
518–82-1	emodin	EMO	*in silico* docking to MCT8	Shaji, 2018
115–09-3	methyl mercury	MeHg	possible MCT8 binding	de Souza et al., 2013
583–39-1	2-mercaptobenzimidazole	MBI	TPO inhibitor	Ramhøj et al., 2021
420–04-2	cyanamide	CYN	TPO inhibitor	Ramhøj et al., 2021
61–82-5	amitrole	AMI	TPO inhibitor	Ramhøj et al., 2021
80–05-7	bisphenol-A	BPA	positive control	Dong and Wade, 2017
80–09-1	bisphenol-S	BPS	BPA-like	
620–92-8	bisphenol-F	BPF	BPA-like	
843–55-0	bisphenol-Z	BPZ	BPA-like	
1478-61-1	bisphenol-AF	BPAF	BPA-like	
152–11-4	verapamil	VRP	MCT8 inhibition	Chen et al., 2022b
57–66-9	probenecid	PRB	OATP inhibitor	Braun et al., 2011

thoroughly. Absorption at 340 nm was measured after 60 min (RT, Multiskan™ FC Microplate Photometer, Thermo Fisher Scientific). Cell viability was expressed as a percentage of vehicle control. Any significant decrease from vehicle control was considered cytotoxic.

2.8. Data analysis

The rate constants for the SK reaction were estimated by a first order kinetic non-linear regression of the measured OD as a function of time. For the estimation of iodide recovery, measured rate constants for digested T3 and T4 were interpolated in the iodide calibration curve that was estimated by a linear regression of observed rate constants as a function of the iodide concentrations. Recoveries were estimated by comparison of the observed to the expected TH concentrations assuming 100% digestion. In the uptake experiments, rate constants of the cell lysates were interpolated in a T3 calibration curve, which was determined in each test plate based on the rate constants of a digested T3 concentration series. Statistically significant differences between the TH uptake in MDCK-MCT8 and MDCK-WT, in the absence or presence of inhibitor, were estimated by two-way ANOVA. For the range-finding study, all results were expressed as percentage of vehicle control and normalized to the positive control (10 μM SY) as the lower limit, by substraction of the positive control mean, and the vehicle control as the upper limit. Chemicals that decreased T3 uptake below 80% of the vehicle control (*i.e.* 20% inhibition) were considered positive hits. Concentration-response regression analysis for the inhibited T3 uptake was performed according to the best-fit approach (Scholze et al., 2001), where multiple non-linear regression models are fitted to the same data set to select a best-fit model. Uptake values were always normalized to the median responses of the vehicle control and the positive control (10 μM SY) on a plate-to-plate basis. In case the three lowest test concentrations provided non-discriminable responses (assessed by linear trend analysis by least squares, $\alpha = 5\%$) but differed statistically significantly from the responses of the vehicle control (Dunnett's multiple comparison test, $\alpha = 5\%$, two-sided), the vehicle controls were discarded and replaced by the three lowest test concentrations for the data normalization ("control re-normalization", Krebs et al., 2018). All concentration-response data analyses were performed with the plate median response as statistical unit, *i.e.* data variability indicates inter-study variation from at least three independent experiments. Chemical-specific potencies were derived from the regression analysis on the control-normalized effect responses and expressed as benchmark concentration (BMC), with the benchmark response level (BMR) determined on basis of all experiments as 1.5 times the between-experimental standard deviation of the replicate medians of the three lowest test concentrations. Median values for the vehicle control cannot be used to determine inter-study variation, because the median of the vehicle controls per plate is always 100% on the normalized effect scale. This BMR corresponds to an 80% intake of that from the vehicle controls (*i.e.* 20% inhibition) and was considered for the given experimental design as most close to the control level for a robust BMC estimation. Statistical analysis were performed using GraphPad Prism version 8 for Windows (GraphPad Software, San Diego, California USA) and SAS 9.3 (SAS Institute, Cary NC).

3. Results

3.1. Iodide recovery of the APS and UV-light digestion methods

To elucidate the effect of the different digestion methods, the release of iodide from TH was compared between the APS-based and the UV-light digestion method. The amount of iodide released from different concentrations of both T3 and T4 after digestion by either APS or UV-light was determined by means of the rate constants of the SK reaction. A standard curve was determined by performing a linear regression on the rate constants as a function of the concentration of T3 (Fig. 1A) and T4 (Fig. 1B). The slope for the T3 standard curve was slightly higher with the UV-light digestion method ($Y = 0.005874*X$) compared to after APS digestion ($Y = 0.005184*X$), but only marginally. There was no difference between the slopes of the T4 standard curve ($Y =$

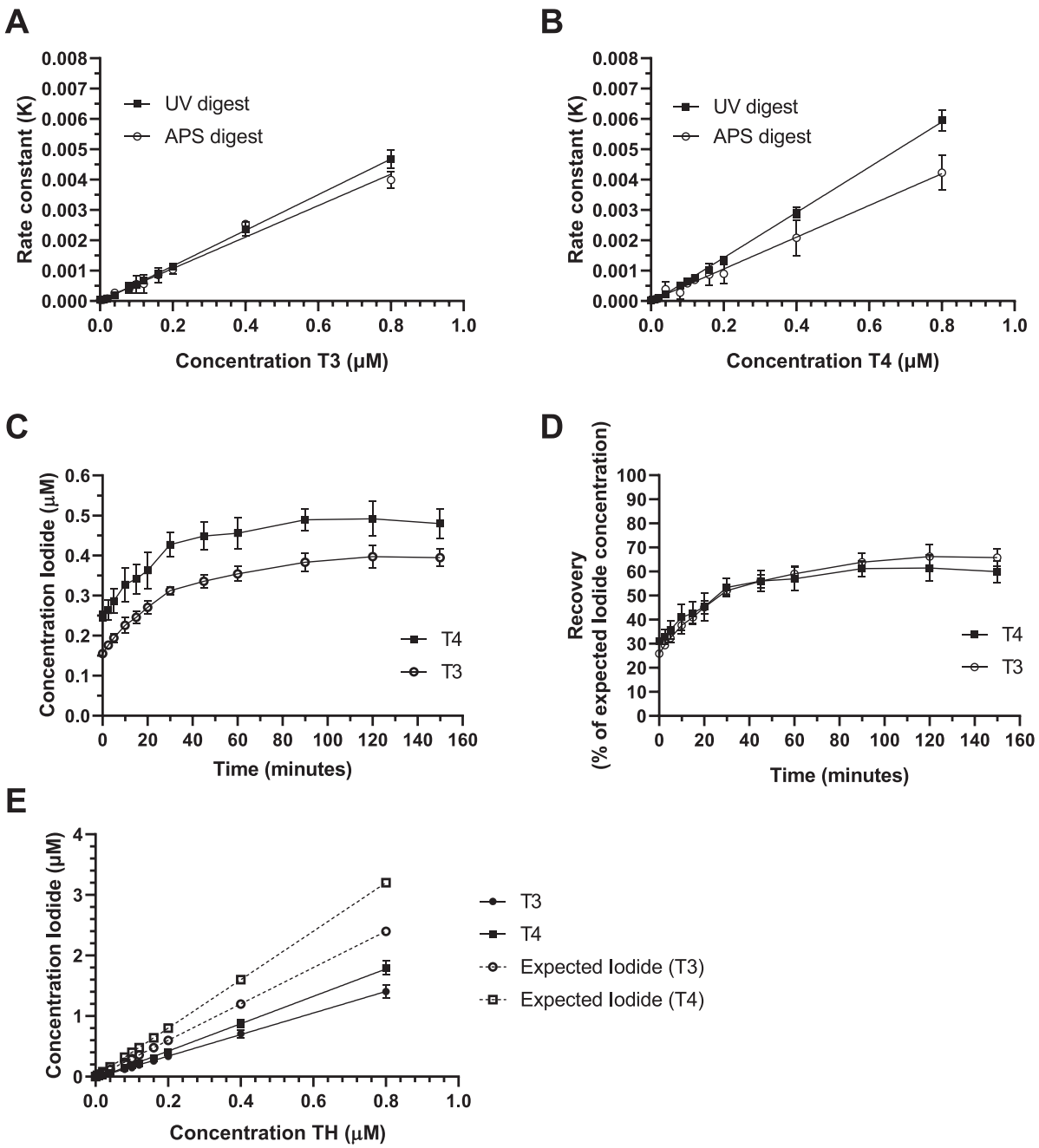

Fig. 1. A) The rate constants of different concentrations of T3 (5× diluted) after digestion with either APS (open) and UV-light based digestion (black). B). The rate constants of different concentrations of T4 (5× diluted) after digestion with either APS (open) and UV-light-based digestion (black). C) Concentration of iodide recovered from 1 μM T3 and 1 μM T4 by UV-light digestion method at different incubation times with UV-light. D) Percentage of recovery of free iodide from 1 μM T3 and 1 μM T4 by UV-light digestion method. E) Recovered iodide concentrations from different concentrations of T3 and T4 (5× diluted) after 90 min UV-light digestion. The expected concentration of iodide for both T3 and T4 in case of 100% digestion efficiency is shown as dashed line. Results are shown as mean ± SD, $N = 3$, p value below 0.05.

0.005234*X) when compared to the slope of the T3 standard curve with the APS-based digestion method. However, there was a ~ 1.3-fold difference between the slope of the T4 standard curves (Y = 0.007457*X) compared to the T3 standard curve after UV-light digestion, reflecting the 4:3 ratio of iodine groups in T4 to T3 (Fig. 1A and B). This fold-difference was also evident when comparing the slope of the T4 standard curves derived from the UV-light digestion method with the slope of the T4 standard curve from the APS-digestion method. To further elucidate the properties of the UV-light digestion method, the recovery of a single concentration of 1 μM (*i.e.* corresponding to an expected ~10% TH uptake from the exposure medium found in pilot experiments) TH was tested at different irradiation times. For both T3 and T4 a higher amount of iodide was measured with increasing UV-light exposure times (Fig. 1C). The recovery of iodide was very similar for both TH and no further increase in the recovery was observed after 90 min of irradiation (Fig. 1D). All further experiments were therefore conducted with an irradiation time of 90 min. The derived amount of iodide from different concentrations of T3 and T4 was also compared to the expected amount of iodide assuming 100% digestion (Fig. 1E). The percentage of recovered iodide ranged between 45 and 60% for both T3 and T4 across all concentrations. The amount of iodide released from T3 and T4 at any concentration was reflected in a 3:4 ratio.

3.2. Applicability of UV-light digestion with MCT8 overexpressing MDCK cells

To demonstrate the compatibility of the UV-light digestion method with cell systems, we tested the UV-light digestion method in combination with MCT8 overexpressing MDCK cell lines previously used with the SK-based TH uptake assay. The uptake of 10 μM T3 at different incubation times was measured in both MDCK-MCT8 and MDCK-WT cells using the modified method with UV-light digestion. In MDCK-MCT8 cells uptake of T3 increased largely linearly over time up to 40 min (Fig. 2). T3 uptake in MDCK-WT cells did also increase over time albeit significantly lower than by MDCK-MCT8 cells. After 40 min incubation MDCK-MCT8 cells had an ~8-fold increase in T3 uptake compared to MDCK-WT cells (Fig. 2B). Moreover, T3 uptake in MDCK-MCT8 cells exposed to 10 μM of the MCT8 specific inhibitor SY (Johannes et al., 2016) was similar as in MDCK-WT cells. These results demonstrate that the UV-light digestion method is capable of digesting T3 in cell systems and that the modified non-radioactive TH uptake assay can be used to screen for potential EDCs.

3.3. EDC screening for MCT8 inhibition

A total of 31 chemicals (Table 1) were tested with the modified non-radioactive TH uptake assay. The uptake of 10 μM T3 in MDCK-MCT8 cells was measured at concentrations of 10 or 100 μM of the test chemical in order to screen for potential EDCs (Fig. 3). All results are shown as the uptake percentage normalized to the vehicle control (0.1% DMSO). Out of the four negative chemicals that were previously reported not to inhibit MCT8-mediated T3 uptake (Table 1), 10 μM of DAID or BP-2 did not inhibit the uptake of T3 in MDCK-MCT8 cells, but 10 μM of XN or TBBPA reduced the uptake of T3 to ~21% and ~ 52%, respectively. All positive chemicals that were previously reported to inhibit T3 uptake *via* MCT8 using non-radioactive assays were also active in our assay. This includes, in order of maximal inhibition: 10 μM SY (~0% remaining T3 uptake), 100 μM ICG (~0%), 100 μM SUNI (~10%), 20 μM DASA (~31%), 100 μM PHL (~33%), 100 μM BSP (~55%), and 100 μM DMI (~61%). Additionally, a significant reduction in T3 uptake was observed for 100 μM BPAF (~15%), 10 μM TBBPA (~21%), 100 μM BPZ (~31%), 100 μM BPA (~44%), 100 μM VRP (~35%), 100 μM PCP (~51%), 10 μM XN (~52%), 10 μM MeHg (~52%), 100 μM PFOS (~59%), 100 μM DIC (~60%) and BPF (~75%). In total 18 out of 31 chemicals tested showed a significant reduction in T3 uptake.

The 15 most potent chemicals that significantly reduced uptake of T3 in the range finding study were further tested to obtain a complete concentration-response pattern (Fig. 4). Only SY, SUNI, DASA, PHL, BSP, BPZ, XN, PCP and TBBPA showed cytotoxic effects at the measured concentrations (supplementary fig. S3). For all other chemicals no cytotoxic effects were observed (data not shown). None of the chemicals showed any cytotoxic effects in the LDH assay (data not shown). The BMC20 (defined as 20% reduction in T3 uptake) was used as lowest inhibitory concentration that could be estimated from the data with sufficient statistical confidence. ICG was the most potent MCT8 inhibitor (BMC = 0.06 μM), followed by SY (0.14 μM), DMI (0.28 μM), MeHg (2.03 μM), PCP (6.06 μM), DASA (6.81 μM), BPZ (11.2 μM), BPAF (18.1 μM), VRP (26.9 μM) and BPA (49.6 μM). Only SY and ICG reached a complete inhibition at non-cytotoxic concentrations, while with DMI, MeHg and PCP the maximal inhibition observed did not exceed 50%. The BMC20 for SUNI, PHL, XN and TBBPA was estimated to occur at cytotoxic concentrations, making it impossible to discern T3 uptake inhibition from cytotoxic effects. The mathematical best-fit regression model together with the BMC20, the lowest cytotoxic concentration (IC20) and number of independent experiments are summarized in Table 2.

4. Discussion

In this study we expanded the previously established MCT8 TH uptake assay by introducing an alternative digestion step which is based on UV-light irradiation rather than APS digestion. UV irradiation has previously been used in the deiodination of T4 and T4 analogues through non-enzymatic photolysis, releasing iodide (van der Walt and Cahnmann, 1982). Although the reaction speed (slope) was slightly higher after UV-light digestion compared to APS-digestion, this increase is most likely negligible when used to interpolate T3 concentrations from unknown samples. As such there is no difference in the sensitivity between APS and UV-light digestion in TH uptake assays that are primarily focused on T3 as a substrate. In conclusion, the UV-light digestion provides an equivalent alternative method to APS digestion that can be used without a laboratory oven, preventing the heating of samples, but requiring specific equipment. Furthermore, TH digestion with the UV-light based digestion step reflects the 3:4 ratio between iodine groups in T3 and T4. This could benefit the sensitivity in TH uptake assays, where T4 is used as a substrate and signal is close to the limit of detection.

The UV-light digestion method was also well suited to measure cellular uptake of T3 when used in combination with the MCT8-MDCK cell line. T3 uptake in the MCT8-MDCK cells increased in time as expected, but did not reach saturation within a 40 min test period. Other

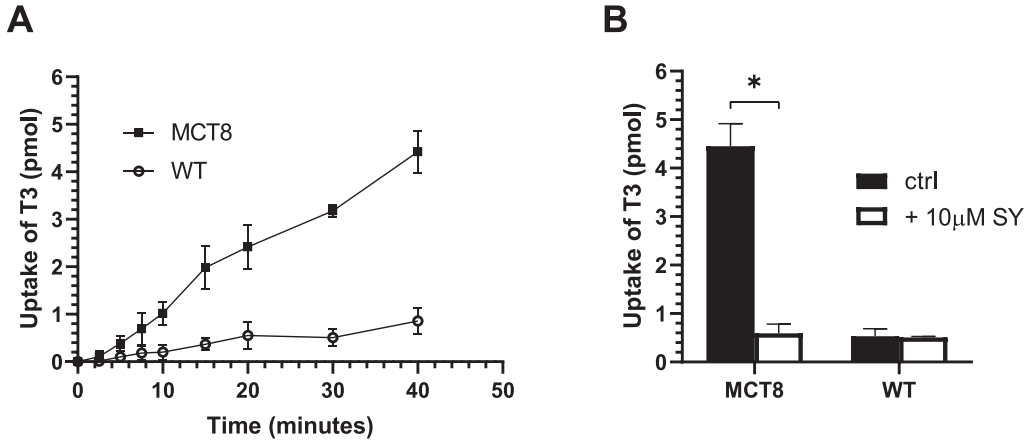

Fig. 2. A) Kinetics of T3 uptake (10 μM) in MDCK-MCT8 or MDCK-WT cells over time. T3 uptake increased steadily over time in MCT8-MDCK cells, while uptake in MDCK-WT cells was negligible. B) Uptake of 10 μM T3 in MDCK-MCT8 and MDCK-WT after 40 min with and without 10 μM SY. MDCK-MCT8 has an 8-fold higher uptake of T3 compared to MDCK-WT cells. Addition of 10 μM SY inhibited the T3 uptake of MDCK-MCT8 cells to MDCK-WT levels. Results are shown as mean ± SD, $N = 3$. p values below 0.05.

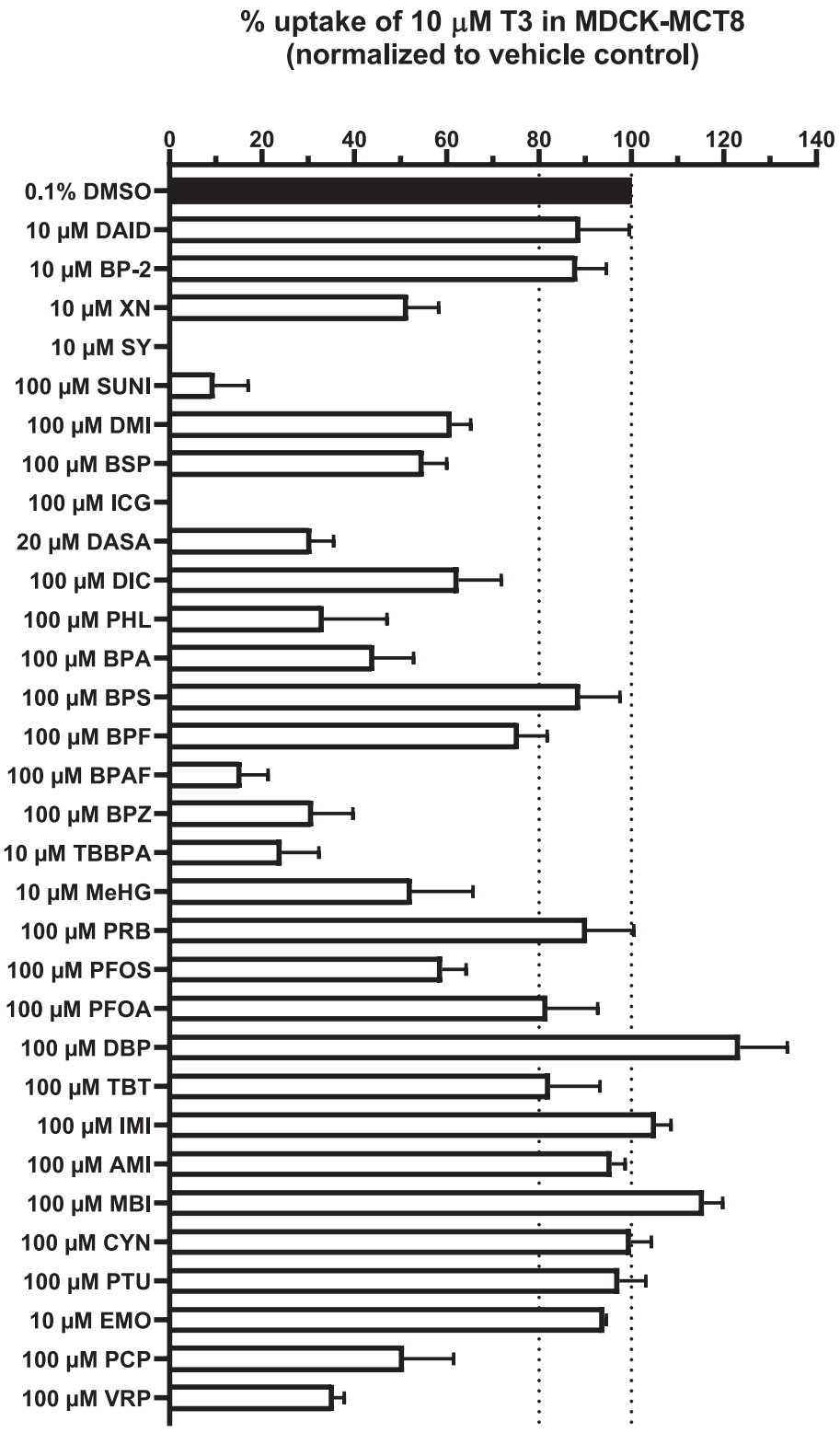

Fig. 3. Percentage of T3 uptake in MCT8-MDCK after exposure to 10 or 100 μM test chemicals compared to vehicle control. Cells were incubated for 30 min with 10 μM T3. Among all chemicals tested XN, SY, SUNI, ICG, BSP, DMI, DASA, PHL, MeHG, BPA, BPAF, BPZ, BPF, VRP, PCP, PFOS, DIC and TBBPA showed significant reduction in T3 uptake compared to vehicle control. 10 μM SY was used a positive control. Results are shown as mean ± SD, $N = 3$. p values below 0,05.

studies using the same cells (Dong and Wade, 2017; Jayarama-Naidu et al., 2015; Kinne et al., 2010) did reach saturation within 30 min. This discrepancy might be attributed to the higher number of cells (20,000 cells per well) used in this study compared to the previously published literature (10,000 cells per well). We also observed full saturation in an experiment with 10,000 cells per well (data not shown), but decided to increase the number of cells to 20,000 cells per well in order to increase the robustness and dynamic range of the assay for further inhibition studies. Ten reference chemicals, with a known effect on T3 uptake by MCT8, were tested with the modified TH uptake assay and responded

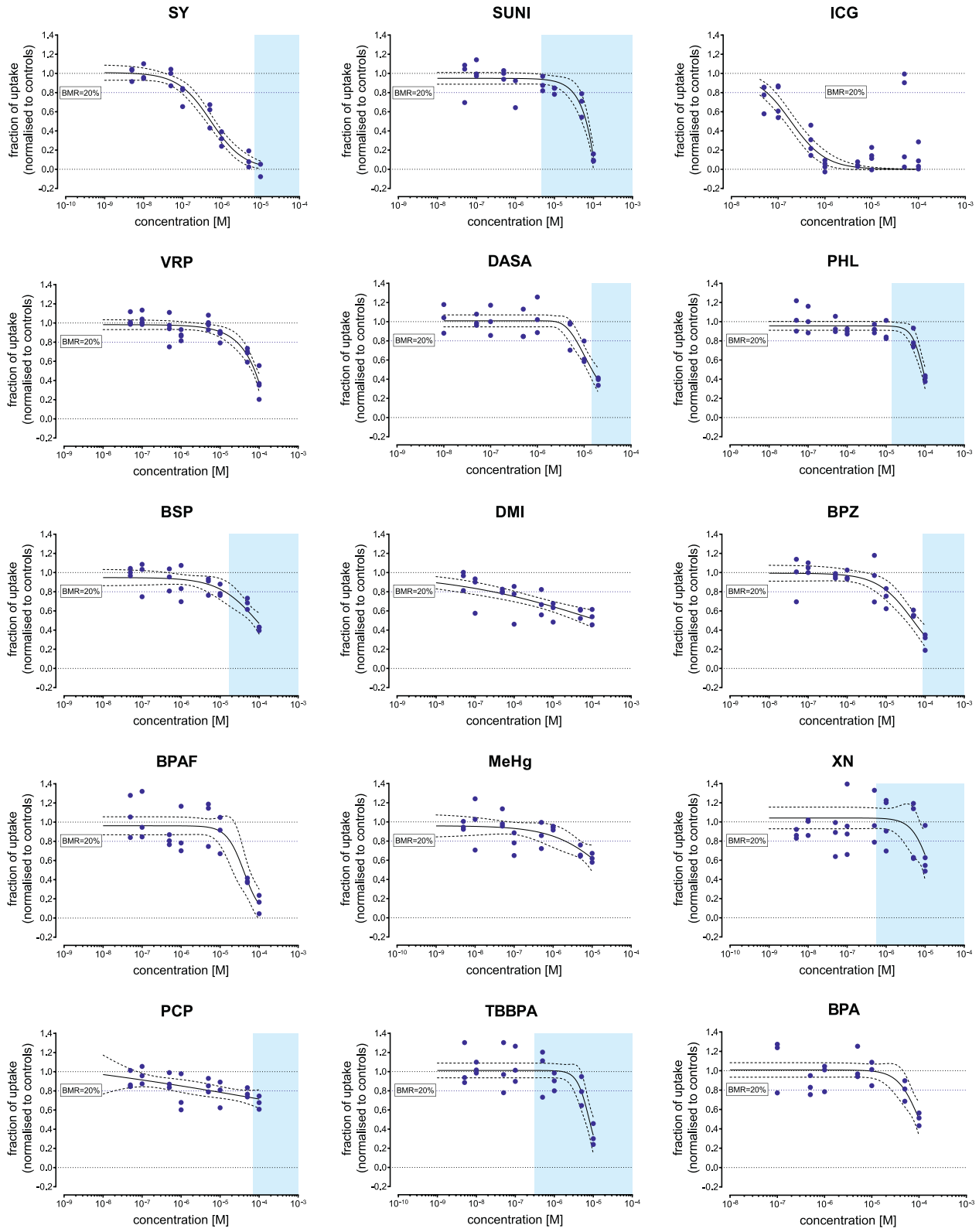

Fig. 4. Concentration-response curves for all test chemicals that showed MCT8 inhibition in MDCK-MCT8. The fraction of T3 uptake is normalized to the DMSO control (upper limit = 1.0) and to the positive control (lower limit = 0.0). SY (10 μM) was used a positive control. All control and chemical concentrations were tested in triplicates per plate, blue dots indicate the plate medians from three to four independent experiments. The black line indicates the best-fit concentrations response curve, the dotted line the corresponding 95% confidence interval, and the BMC20, the concentration that inhibits the T3 uptake by 20%. A blue box indicates the concentration range at which cytotoxicity was measured in the resazurine assay, with the IC20 set as the lowest value. (For interpretation of the references to colour in this figure legend, the reader is referred to the web version of this article.)

Table 2
Inhibition of T3 uptake and cytotoxicity of individual chemicals in the MDCK-MCT8 uptake assay.

Substance (by order of BMC20)	Concentration Response Function						T3 uptake inhibition		Cytotoxicity[1)]
	N_{study}	RM	$\hat{\theta}_1$	$\hat{\theta}_2$	$\hat{\theta}_{min}$	$\hat{\theta}_{max}$	BMC20 (M), [CI]	IC50 [M]	IC20 (M)
indocyanine green	4	logit	−18.11	−2.69	0*	1*	5.73E-08 [3.52E-08; 9.30E-08]	1.87E-07	> 1.00E-04
silychristin	3	logit	−14.84	−2.36	0*	1.01	1.43E-07 [9.06E-08; 2.24E-07]	5.37E-07	7.07E-06 (3.65E-07 - 1.37E-04)
desipramide	3	logit	−1.98	−0.51	0*	1*	2.84E-07 [5.08E-08; 1.59E-06]	> 0.0001	> 0.001
methyl mercury	3	logit	−6.66	−1.45	0*	0.96	2.03E-06 [5.09E-07; 8.11E-06]	2.28E-05	> 1.00E-05
tetrabromobisphenol A	3	logit	−33.27	−6.51	0*	1.01	4.89E-06 [3.24E-06; 7.37E-06]	7.88E-06	3.09E-07 (1.23E-07 - 7.75E-07)
pentachlorophenol	3	logit	−0.67	−0.22	0*	1.29	6.06E-06 [6.69E-07; 5.50E-05]	No data support	7.03E-05 (2.39E-05 - 1.17E-04)
dasatinib	3	Weibull	−12.49	−2.51	0*	1.01	6.81E-06 [4.89E-06; 9.49E-06]	1.47E-05	1.49E-05 (8.71E-06 - 2.55E-05)
xanthohumol	4	logit	−20.88	−4.28	0*	1.04	6.97E-06 [3.65E-06; 1.33E-05]	1.39E-05	5.75E-07 (2.41E-07 - 1.37E-06)
bisphenol-Z	3	logit	−9.44	−2.19	0*	0.99	1.12E-05 [5.40E-06; 2.32E-05]	2.42E-05	8.76E-05 (4.89E-06 - 1.57E-03)
bromosulfophthalein	3	logit	−7.81	−1.95	0*	0.95	1.33E-05 [4.39E-06; 4.02E-05]	8.57E-05	1.72E-05 (3.68E-06 - 8.07E-05)
bisphenol-AF	3	logit	−19.65	−4.48	0*	0.96	1.81E-05 [6.95E-06; 4.71E-05]	2.06E-05	> 0.001
verapamil	4	logit	4.16	−2.11	−176,476	0.98	2.69E-05 [1.61E-05; 4.50E-05]	7.80E-05	>0.0001
sunitinib malate	3	logit	−0.51	−3.29	−257,345	0.95	3.01E-05 [1.73E-05; 5.25E-05]	6.53E-05	4.63E-06 (2.33E-06 - 9.21E-06)
bisphenol-A	3	logit	−17.78	−4.44	0*	1.01	4.96E-05 [2.89E-05; 8.50E-05]	1.01E-04	> 0.001
phloretin	3	logit	−27.38	−6.77	0*	0.96	5.20E-05 [3.83E-05; 7.07E-05]	8.78E-05	1.38E-05 (4.82E-06 - 3.95E-05)

BMC20: concentration that inhibits the T3 uptake by 20%; IC50: concentration that inhibits the T3 uptake by 50% (estimated); IC20: concentration that inhibits cell viability by 20% in the resazurin cell viability assay[1]. Values in brackets denote the upper and lower limits of the approximate 95% confidence interval (CI); the column "RM" indicates the mathematical regression function as defined by Scholze et al. (2001): $\hat{\theta}_1, \hat{\theta}_2, \hat{\theta}_{min}, \hat{\theta}_{max}$ estimated model parameters, given for concentrations expressed in M (rounded values), with * highlighting parameters that were not estimated but set to a fixed value. N_{study} = number of independent experiments.
[1] indicated as blue boxes in Fig. 4.

similarly as reported in previously published studies (Johannes et al., 2016; Dong and Wade, 2017). As expected, negative control chemicals DAIZ and BP2 did not affect T3 uptake in our assay. The other negative control chemicals XN and TBBPA did affect T3 uptake, but at cytotoxic concentrations. Johannes et al. (2016) found no inhibitory effect in the non-radioactive TH uptake assay at a concentration of 10 μM, but cells were only exposed for 15 min to the inhibitors and test chemicals. Similarly, Dong and Wade (2017) in their MCT8 screening also incubated for 15 min with TBBPA and found no cytotoxic effects. Therefore, it is likely that the decrease in T3 uptake observed in our assay is due to cytotoxic effects after 30 min of incubation and not due to an inhibition of MCT8-mediated T3 transport. Additionally, all chemicals that were previously reported to inhibit T3 uptake were also shown to inhibit T3 uptake in our assay. Chen et al. (2022b) described VRP as a weak MCT8 inhibitor using radiolabeled isotopes in transiently transfected COS-1 cells. VRP also inhibited T3 uptake in our test system at concentrations higher than 27 μM. MCT8-mediated T3 uptake was also inhibited by DASA, BPA and DMI. PHL, BSP and SUNI inhibited T3 uptake only at cytotoxic concentrations. Consistent with our data, both ICG and SY were previously reported to be potent MCT8 inhibitors, whereas BPA was only considered to be a weak MCT8 inhibitor (Dong and Wade, 2017; Johannes et al., 2016). The high accordance between our data and published results shows that the modified TH uptake assay is well suited for the detection of potential EDCs.

We further applied the modified TH uptake assay to screen 22 environmentally relevant chemicals for potential endocrine disrupting effect on MCT8. We identified MeHg, PCP, BPAF, BPZ, PFOS, DIC and BPF as MCT8 inhibiting chemicals that were not previously reported. de Souza et al. 2013 reported that mercury containing chemicals inhibit T3 uptake by binding to cysteine residues in MCT8. Here we confirmed that MeHg can also acts upon MCT8 facilitated T3 uptake, possibly through a similar mechanism. Interestingly, MeHg intoxication and hypothyroidism share very similar neurodevelopmental pathology, suggesting a possible role for TH modulation by MeHg poisoning (Soldin et al., 2008). In a recent meta-analysis, mercury concentrations in blood have also been positively associated with TSH and free T4 (FT4) concentrations, but no significant association was found with (free) T3 (Hu et al., 2021). MeHg has also been associated with a decrease of DIO2 functionality and TH synthesis at much lower concentrations than in our TH uptake assay (Kawada et al., 1980; Mori et al., 2006). Heavy metal cations such as Hg+, Cd2+ or Pb2+ will irreversibly inactivate their function and also impair the essential redox-control by other selenoproteins required for TH biosynthesis of the thyroid gland (Köhrle, 2023). Aside from evidence that exposure to MeHg may impair the TH system, several other modes of action that are independent of TH signaling have also been proposed as a cause of MeHg-associated neurotoxicity (Aaseth et al., 2020). Nonetheless, mercury-containing compounds remain an interesting group of contaminants to investigate with regards to TH homeostasis, metabolism and action. Additionally, we demonstrated that bisphenols BPAF, BPZ and BPF are weak MCT8 inhibitors in addition to the previously reported BPA (Dong and Wade, 2017), while no inhibition was observed for BPS. BPA is by far the most widely studied bisphenol with regards to TH concentrations. The effects of BPA exposure on TH serum concentrations are not clear (Kim and Park, 2019; Koutaki et al., 2022). In a large cohort of pregnant woman, BPA and BPF, but not BPS, have been positively associated with increased maternal serum free T3 concentrations, but these associations only existed until gestational week 12 (Derakhshan et al., 2019). In contrast, other studies have reported that maternal BPA exposure is positively associated with decreased free T3 and total T4 in cord blood, but no associations were found for BPS, BPF or BPAF (Xi et al., 2023). All the bisphenols examined in this study are also known to cause significant gene transcription changes in TH regulating genes in rat pituitary and thyroid follicular cells, generally decreasing the expression of TH receptors and deiodinases (Lee et al., 2017). Interestingly, both TH and bisphenols are composed of two phenolic rings, which might explain the overlap in activities. Bisphenols could very well interfere with TH signaling, although the serum concentrations reported *in vivo* are likely to be much lower than concentrations used in this study. For example, BPA concentrations have been reported in maternal and cord serum ranges between 1 and 2 ng/mL (Derakhshan et al., 2021; J. Lee et al., 2018; Xi et al., 2023).

Translating *in vitro* data to *in vivo* markers for EDC effects remains difficult. Typically, rodent or mouse models are used to assess the effect of EDCs on TH signaling and adverse outcomes. However, THS disrupting effects seen in rodent and mouse models do not always reflect the human situation. For TH transport mediated effects, for example, the expression of THTMT differs greatly between species (Vancamp and Darras, 2018). A clear example of this is shown in MCT8-deficient mice models, where mice with engineered non-functional MCT8 lack severe neurological impairments that are observed in human MCT8-deficient patients, despite showing a strong diminished T3 uptake in the brain (Trajkovic et al., 2007; Wirth et al., 2009). This is partly attributed to the existence of other THTMT that provides possible compensatory alternative routes of TH uptake for MCT8-deficient mice. Indeed, mice lacking both MCT8 and

OATP1C1 have more strongly diminished TH content in the brain and represent the adverse phenotype of MCT8-deficient humans better than MCT8 deficient mice and represent a valid model for the AHDS phenotype (Mayerl et al., 2014). In chickens, distribution and expression of TH transporters as well as deiodinases is differently arranged in the compartmental barriers, with MCT8 exclusively expressed in the embryonic BCSFB, but not in brain capillary endothelial cells (van Herck et al., 2015). These interspecies differences should be considered when selecting a relevant *in vivo*, *in silico* and *in vitro* models for the specific research question of interest. To prevent differences in phenotypic adverse effects due to compensatory routes of TH uptake, knockout animal models, for instance OATP1C1 knockout mice, could be used to study *in vivo* effects of MCT8 specific inhibitors. Additionally, discussions about the relevance of serum TH concentrations as indicators of neurodevelopmental adverse effects further highlight that not only relevant models, but also relevant parameters need to be considered for TH related toxicological studies (Gilbert et al., 2020). TH concentrations in brain, for instance, are a better indicator for neurodevelopmental adverse effects by THTMT inhibiting chemicals or deiodinase inhibitors than TH concentrations in serum. Therefore, mechanistic data on the mode of action of EDCs affecting TH signaling, particularly those of molecular initiating events, are needed to provide crucial information for *in vivo* studies for THS disrupting chemicals. Moreover, data from *in vitro* studies on the mode of action of EDCs can help in the prioritization of EDCs to be tested in further toxicological studies.

In conclusion, we explored the use of an alternative UV-light digestion method of TH to proceed the Sandell-Kolthoff reaction. We furthermore applied this alternative digestion method in an existing TH uptake assay in combination with a cell line overexpressing MCT8 to screen a relevant set of 30 chemicals, identifying MeHg, BPAF and BPZ as novel MCT8 inhibitors. Our results suggest that the modified TH uptake assay can be used to screen potential EDCs easily and rapidly for their effect on T3 uptake *via* MCT8.

Funding

This work was funded by the EU Horizon 2020 project ATHENA: Assays for the identification of Thyroid Hormone axis-disrupting chemicals, under grant number 82516.

CRediT authorship contribution statement

Fabian Wagenaars: Conceptualization, Investigation, Methodology, Visualization, Writing – original draft. **Peter Cenijn:** Conceptualization, Investigation, Methodology, Writing – review & editing. **Martin Scholze:** Formal analysis, Writing – review & editing. **Caroline Frädrich:** Writing – review & editing, Resources. **Kostja Renko:** Writing – review & editing, Resources. **Josef Köhrle:** Resources, Writing – review & editing. **Timo Hamers:** Funding acquisition, Project administration, Supervision, Writing – review & editing.

Declaration of Competing Interest

The authors declare no conflict of interests.

Data availability

Data will be made available on request.

Acknowledgements

The authors want to thank Ulrich Schweizer and Doreen Braun from the University of Bonn for providing the MDCK-MCT8 cell lines. Furthermore, we appreciate the help of Marcel Meima, Zhongli Chen and Robin Peeters for their comments and continued practical support during the production of this manuscript.

Appendix A. Supplementary data

Supplementary data to this article can be found online at https://doi.org/10.1016/j.tiv.2023.105770.

References

Aaseth, J., Wallace, D.R., Vejrup, K., Alexander, J., 2020. Methylmercury and developmental neurotoxicity: A global concern. In: Current Opinion in Toxicology, vol. 19. Elsevier B.V, pp. 80–87. https://doi.org/10.1016/j.cotox.2020.01.005.

Andersen, S.L., Andersen, S., 2021. Hyperthyroidism in pregnancy: Evidence and hypothesis in fetal programming and development. In: Endocrine Connections (Vol. 10, Issue 2, pp. 77–86). BioScientifica Ltd. https://doi.org/10.1530/EC-20-0518

Braun, D., Kinne, A., Brauer, A.U., Sapin, R., Klein, M.O., Köhrle, J., Wirth, E.K., Schweizer, U., 2011. Developmental and cell type-specific expression of thyroid hormone transporters in the mouse brain and in primary brain cells. GLIA 59 (3), 463–471. https://doi.org/10.1002/glia.21116.

Braun, D., Kim, T.D., le Coutre, P., Köhrle, J., Hershman, J.M., Schweizer, U., 2012. Tyrosine kinase inhibitors noncompetitively inhibit MCT8-mediated iodothyronine transport. J. Clin. Endocrinol. Metab. 97 (1) https://doi.org/10.1210/jc.2011-1837.

Buckalew, A.R., Wang, J., Murr, A.S., Deisenroth, C., Stewart, W.M., Stoker, T.E., Laws, S.C., 2020. Evaluation of potential sodium-iodide symporter (NIS) inhibitors using a secondary Fischer rat thyroid follicular cell (FRTL-5) radioactive iodide uptake (RAIU) assay. Arch. Toxicol. 94 (3), 873–885. https://doi.org/10.1007/s00204-020-02664-y.

Chen, Z., Meima, M.E., Peeters, R.P., Visser, W.E., 2022a. Thyroid hormone transporters in pregnancy and fetal development. In: *International Journal of Molecular Sciences* (Vol. 23, issue 23). MDPI. https://doi.org/10.3390/ijms232315113.

Chen, Z., van der Sman, A.S.E., Groeneweg, S., de Rooij, L.J., Visser, W.E., Peeters, R.P., Meima, M.E., 2022b. Thyroid hormone transporters in a human placental cell model. Thyroid. https://doi.org/10.1089/thy.2021.0503.

Derakhshan, A., Shu, H., Peeters, R.P., Kortenkamp, A., Lindh, C.H., Demeneix, B., Bornehag, C.G., Korevaar, T.I.M., 2019. Association of urinary bisphenols and triclosan with thyroid function during early pregnancy. Environ. Int. 133 https://doi.org/10.1016/j.envint.2019.105123.

Derakhshan, A., Philips, E.M., Ghassabian, A., Santos, S., Asimakopoulos, A.G., Kannan, K., Kortenkamp, A., Jaddoe, V.W.V., Trasande, L., Peeters, R.P., Korevaar, T.I.M., 2021. Association of urinary bisphenols during pregnancy with maternal, cord blood and childhood thyroid function. Environ. Int. 146 https://doi.org/10.1016/j.envint.2020.106160.

Dong, H., Wade, M.G., 2017. Application of a nonradioactive assay for high throughput screening for inhibition of thyroid hormone uptake via the transmembrane transporter MCT8. Toxicol. in Vitro 40, 234–242. https://doi.org/10.1016/j.tiv.2017.01.014.

Friedman, K.P., Watt, E.D., Hornung, M.W., Hedge, J.M., Judson, R.S., Crofton, K.M., Houck, K.A., Simmons, S.O., 2016. Tiered high-throughput screening approach to identify thyroperoxidase inhibitors within the toxcast phase I and II chemical libraries. Toxicol. Sci. 151 (1), 160–180. https://doi.org/10.1093/toxsci/kfw034.

Friesema, E.C.H., Kuiper, G.G.J.M., Jansen, J., Visser, T.J., Kester, M.H.A., 2006. Thyroid hormone transport by the human monocarboxylate transporter 8 and its rate-limiting role in intracellular metabolism. Mol. Endocrinol. 20 (11), 2761–2772. https://doi.org/10.1210/me.2005-0256.

Gilbert, M.E., Rovet, J., Chen, Z., Koibuchi, N., 2012. Developmental thyroid hormone disruption: Prevalence, environmental contaminants and neurodevelopmental consequences. NeuroToxicology 33 (4), 842–852. https://doi.org/10.1016/j.neuro.2011.11.005.

Gilbert, M.E., O'Shaughnessy, K.L., Axelstad, M., 2020. Regulation of thyroid-disrupting chemicals to protect the developing brain. In: *Endocrinology (United States)* (Vol. 161, issue 10). Endocrine Society. https://doi.org/10.1210/endocr/bqaa106.

Groeneweg, S., van Geest, F.S., Peeters, R.P., Heuer, H., Visser, W.E., 2019. Thyroid hormone transporters. In: *Endocrine Reviews* (Vol. 41, issue 2). Endocrine Society. https://doi.org/10.1210/endrev/bnz008.

Hamers, T., Kamstra, J.H., Sonneveld, E., Murk, A.J., Kester, M.H.A., Andersson, P.L., Legler, J., Brouwer, A., 2006. In vitro profiling of the endocrine-disrupting potency of brominated flame retardants. Toxicol. Sci. 92 (1), 157–173. https://doi.org/10.1093/toxsci/kfj187.

Hu, Q., Han, X., Dong, G., Yan, W., Wang, X., Bigambo, F.M., Fang, K., Xia, Y., Chen, T., Wang, X., 2021. Association between mercury exposure and thyroid hormones levels: a meta-analysis. Environ. Res. 196 https://doi.org/10.1016/j.envres.2021.110928.

Illouz, F., Braun, D., Briet, C., Schweizer, U., Rodien, P., 2014. Endocrine side-effects of anti-cancer drugs: thyroid effects of tyrosine kinase inhibitors. In: *European journal of endocrinology* (Vol. 171, issue 3, pp. R91–R99). BioScientifica Ltd. https://doi.org/10.1530/EJE-14-0198.

Ishihara, A., Sawatsubashi, S., Yamauchi, K., 2003. Endocrine disrupting chemicals: interference of thyroid hormone binding to transthyretins and to thyroid hormone receptors. Mol. Cell. Endocrinol. 199, 105–117. www.elsevier.com/locate/mce.

Jayarama-Naidu, R., Johannes, J., Meyer, F., Wirth, E.K., Schomburg, L., Köhrle, J., Renko, K., 2015. A nonradioactive uptake assay for rapid analysis of thyroid hormone transporter function. Endocrinology (United States) 156 (7), 2739–2745. https://doi.org/10.1210/en.2015-1016.

Johannes, J., Jayarama-Naidu, R., Meyer, F., Wirth, E.K., Schweizer, U., Schomburg, L., Köhrle, J., Renko, K., 2016. Silychristin, a flavonolignan derived from the milk

thistle, is a potent inhibitor of the thyroid hormone transporter MCT8. Endocrinology 157 (4), 1694–1701. https://doi.org/10.1210/en.2015-1933.
Kawada, J., Nishida, M., Yoshimura, Y., Mitani, K., 1980. Effect of organic and inorganic mercurials on thyroidal functions. Aust. J. Pharm. 3 (3), 149–159.
Kim, M.J., Park, Y.J., 2019. Bisphenols and thyroid hormone. In: *Endocrinology and Metabolism* (Vol. 34, issue 4, pp. 340–348). Korean Endocrine Society. https://doi.org/10.3803/EnM.2019.34.4.340.
Kinne, A., Roth, S., Biebermann, H., Köhrle, J., Grüters, A., Schweizer, U., 2009. Surface translocation and tri-iodothyronine uptake of mutant MCT8 proteins are cell type-dependent. J. Mol. Endocrinol. 43 (6), 263–271. https://doi.org/10.1677/JME-09-0043.
Kinne, A., Kleinau, G., Hoefig, C.S., Grüters, A., Köhrle, J., Krause, G., Schweizer, U., 2010. Essential molecular determinants for thyroid hormone transport and first structural implications for monocarboxylate transporter 8. J. Biol. Chem. 285 (36), 28054–28063. https://doi.org/10.1074/jbc.M110.129577.
Köhrle, J., 2023. Selenium, iodine and Iron–essential trace elements for thyroid hormone synthesis and metabolism. In: *International Journal of Molecular Sciences* (Vol. 24, issue 4). MDPI. https://doi.org/10.3390/ijms24043393.
Köhrle, J., Frädrich, C., 2021. Thyroid hormone system disrupting chemicals. In: *Best Practice and Research: Clinical Endocrinology and Metabolism* (Vol. 35, issue 5). Bailliere Tindall Ltd. https://doi.org/10.1016/j.beem.2021.101562.
Koutaki, D., Paltoglou, G., Vourdoumpa, A., Charmandari, E., 2022. The impact of bisphenol a on thyroid function in neonates and children: a systematic review of the literature. In: *Nutrients* (Vol. 14, issue 1). MDPI. https://doi.org/10.3390/nu14010168.
Krebs, A., Nyffeler, J., Rahnenführer, J., Leist, M., 2018. Normalization of data for viability and relative cell function curves. ALTEX 35 (2). https://doi.org/10.14573/altex.1803231.
Landers, K., Richard, K., 2017. Traversing barriers – how thyroid hormones pass placental, blood-brain and blood-cerebrospinal fluid barriers. Mol. Cell. Endocrinol. 458, 22–28. https://doi.org/10.1016/j.mce.2017.01.041.
Lee, J., Choi, K., Park, J., Moon, H.B., Choi, G., Lee, J.J., Suh, E., Kim, H.J., Eun, S.H., Kim, G.H., Cho, G.J., Kim, S.K., Kim, S., Kim, S.Y., Kim, S., Eom, S., Choi, S., Kim, Y. D., Kim, S., 2018. Bisphenol a distribution in serum, urine, placenta, breast milk, and umbilical cord serum in a birth panel of mother–neonate pairs. Sci. Total Environ. 626, 1494–1501. https://doi.org/10.1016/j.scitotenv.2017.10.042.
Lee, S., Kim, C., Youn, H., Choi, K., 2017. Thyroid hormone disrupting potentials of bisphenol a and its analogues - in vitro comparison study employing rat pituitary (GH3) and thyroid follicular (FRTL-5) cells. Toxicol. in Vitro 40, 297–304. https://doi.org/10.1016/j.tiv.2017.02.004.
Leonard, J.L., 1986. Thyroid hormone metabolism in kidney epithelial cells in continuous culture. In: Frontiers in Thyroidology. Springer US, pp. 437–441. https://doi.org/10.1007/978-1-4684-5260-0_77.
Loubière, L.S., Vasilopoulou, E., Bulmer, J.N., Taylor, P.M., Stieger, B., Verrey, F., McCabe, C.J., Franklyn, J.A., Kilby, M.D., Chan, S.Y., 2010. Expression of thyroid hormone transporters in the human placenta and changes associated with intrauterine growth restriction. Placenta 31 (4), 295–304. https://doi.org/10.1016/j.placenta.2010.01.013.
Mayerl, S., Müller, J., Bauer, R., Richert, S., Kassmann, C.M., Darras, V.M., Buder, K., Boelen, A., Visser, T.J., Heuer, H., 2014. Transporters MCT8 and OATP1C1 maintain murine brain thyroid hormone homeostasis. J. Clin. Investig. 124 (5), 1987–1999. https://doi.org/10.1172/JCI70324.
Mori, K., Yoshida, K., Tani, J.I., Hoshikawa, S., Ito, S., Watanabe, C., 2006. Methylmercury inhibits type II 5′-deiodinase activity in NB41A3 neuroblastoma cells. Toxicol. Lett. 161 (2), 96–101. https://doi.org/10.1016/j.toxlet.2005.08.001.
Noyes, P.D., Friedman, K.P., Browne, P., Haselman, J.T., Gilbert, M.E., Hornung, M.W., Barone, S., Crofton, K.M., Laws, S.C., Stoker, T.E., Simmons, S.O., Tietge, J.E., Degitz, S.J., 2019. Evaluating chemicals for thyroid disruption: Opportunities and challenges with in Vitro testing and adverse outcome pathway approaches. In: *Environmental Health Perspectives* (Vol. 127, Issue 9). Public Health Services, US Dept of Health and Human Services. https://doi.org/10.1289/EHP5297.
Ohashi, T., Yamaki, M., Pandav, C.S., Karmarkar, M.G., Irie, M., 2000. Simple microplate method for determination of urinary iodine. Clin. Chem. 46 (4). https://academic.oup.com/clinchem/article/46/4/529/5641194.
Patzeltová, N., 1993. Determination of microquantities of iodine in biological materials. Chem. Pap. 47 (4), 237–239.
Pino, S., Fang, S.-L., Braverman1, L. E., 1996. Ammonium persulfate: a safe alternative oxidizing reagent for measuring urinary iodine. In Clin. Chem. 42.
Ramhøj, L., Frädrich, C., Svingen, T., Scholze, M., Wirth, E.K., Rijntjes, E., Köhrle, J., Kortenkamp, A., Axelstad, M., 2021. Testing for heterotopia formation in rats after developmental exposure to selected in vitro inhibitors of thyroperoxidase. Environ. Pollut. 283 https://doi.org/10.1016/j.envpol.2021.117135.
Renko, K., Hoefig, C.S., Hiller, F., Schomburg, L., Köhrle, J., 2012. Identification of iopanoic acid as substrate of type 1 deiodinase by a novel nonradioactive iodide-release assay. Endocrinology 153 (5), 2506–2513. https://doi.org/10.1210/en.2011-1863.
Roberts, L.M., Woodford, K., Zhou, M., Black, D.S., Haggerty, J.E., Tate, E.H., Grindstaff, K.K., Mengesha, W., Raman, C., Zerangue, N., 2008. Expression of the thyroid hormone transporters monocarboxylate transporter-8 (SLC16A2) and organic ion transporter-14 (SLCO1C1) at the blood-brain barrier. Endocrinology 149 (12), 6251–6261. https://doi.org/10.1210/en.2008-0378.
Sandell, E.B., Kolthoff, I.M., 1937. Micro determination of iodine by a catalytic method. Microchim. Acta 1, 9–25.
Scholze, M., Boedeker, W., Faust, M., Backhaus, T., Altenburger, R., Horst Grimme, L., 2001. A general best-fit method for concentration-response curves and the estimation of low-effect concentrations. In: *Environmental Toxicology and Chemistry* (Vol. 20, issue 2).
Schwartz, C.E., May, M.M., Carpenter, N.J., Rogers, R.C., Martin, J., Bialer, M.G., Ward, J., Sanabria, J., Marsa, S., Lewis, J.A., Echeverri, R., Lubs, H.A., Voeller, K., Simensen, R.J., Stevenson, R.E., 2005. Allan-Herndon-Dudley syndrome and the Monocarboxylate transporter 8 (MCT8) gene. In. Am. J. Hum. Genet. 77.
Shaji, D., 2018. Molecular docking studies of human MCT8 protein with soy isoflavones in Allan-Herndon-Dudley syndrome (AHDS). J. Pharmaceut. Anal. 8 (5), 318–323. https://doi.org/10.1016/j.jpha.2018.07.001.
Sharan, S., Nikhil, K., Roy, P., 2014. Disruption of thyroid hormone functions by low dose exposure of tributyltin: an in vitro and in vivo approach. Gen. Comp. Endocrinol. 206, 155–165. https://doi.org/10.1016/j.ygcen.2014.07.027.
Shelor, C.P., Dasgupta, P.K., 2011. Review of analytical methods for the quantification of iodine in complex matrices. In: *Analytica Chimica Acta* (Vol. 702, issue 1, pp. 16–36). https://doi.org/10.1016/j.aca.2011.05.039.
Shimada, N., Yamauchi, K., 2004. Characteristics of 3,5,3′-triiodothyronine (T3)-uptake system of tadpole red blood cells: effect of endocrine-disrupting chemicals on cellular T3 response. J. Endocrinol. 183 (3), 627–637. https://doi.org/10.1677/joe.1.05893.
Soldin, O.P., O'Mara, D.M., Aschner, M., 2008. Thyroid hormones and methylmercury toxicity. In: *Biological Trace Element Research* (Vol. 126, issues 1–3, pp. 1–12). https://doi.org/10.1007/s12011-008-8199-3.
de Souza, E.C.L., Groeneweg, S., Visser, W.E., Peeters, R.P., Visser, T.J., 2013. Importance of cysteine residues in the thyroid hormone transporter MCT8. Endocrinology 154 (5), 1948–1955. https://doi.org/10.1210/en.2012-2101.
Trajkovic, M., Visser, T.J., Mittag, J., Horn, S., Lukas, J., Darras, V.M., Raivich, G., Bauer, K., Heuer, H., 2007. Abnormal thyroid hormone metabolism in mice lacking the monocarboxylate transporter 8. J. Clin. Investig. 117 (3), 627–635. https://doi.org/10.1172/JCI28253.
van der Walt, B., Cahnmann, H.J., 1982. Synthesis of thyroid hormone metabolites by photolysis of thyroxine and thyroxine analogs in the near UV (specifically labeled iodothyronines/HPLC). In Proc. NatL Acad. Sci. USA 79.
van Herck, S.L.J., Delbaere, J., Bourgeois, N.M.A., McAllan, B.M., Richardson, S.J., Darras, V.M., 2015. Expression of thyroid hormone transporters and deiodinases at the brain barriers in the embryonic chicken: insights into the regulation of thyroid hormone availability during neurodevelopment. Gen. Comp. Endocrinol. 214, 30–39. https://doi.org/10.1016/j.ygcen.2015.02.021.
Vancamp, P., Darras, V.M., 2018. From zebrafish to human: A comparative approach to elucidate the role of the thyroid hormone transporter MCT8 during brain development. In: General and Comparative Endocrinology, vol. 265. Academic Press Inc., pp. 219–229. https://doi.org/10.1016/j.ygcen.2017.11.023
Vatine, G.D., Al-Ahmad, A., Barriga, B.K., Svendsen, S., Salim, A., Garcia, L., Garcia, V.J., Ho, R., Yucer, N., Qian, T., Lim, R.G., Wu, J., Thompson, L.M., Spivia, W.R., Chen, Z., van Eyk, J., Palecek, S.P., Refetoff, S., Shusta, E.V., Svendsen, C.N., 2017. Modeling psychomotor retardation using iPSCs from MCT8-deficient patients indicates a prominent role for the blood-brain barrier. Cell Stem Cell 20 (6), 831–843.e5. https://doi.org/10.1016/j.stem.2017.04.002.
Tsuda, K., Namba, H., Nomura, T., Yokoyama, N., Yamashita, S., Izumi, M., Nagataki, S., 1995. Automated measurement of urinary iodine with use of ultraviolet irradiation. Clin. Chem. 41 (4), 581.
Weiss, J.M., Andersson, P.L., Lamoree, M.H., Leonards, P.E.G., van Leeuwen, S.P.J., Hamers, T., 2009. Competitive binding of poly- and perfluorinated compounds to the thyroid hormone transport protein transthyretin. Toxicol. Sci. 109 (2), 206–216. https://doi.org/10.1093/toxsci/kfp055.
Westholm, D.E., Stenehjem, D.D., Rumbley, J.N., Drewes, L.R., Anderson, G.W., 2009. Competitive inhibition of organic anion transporting polypeptide 1c1-mediated thyroxine transport by the fenamate class of nonsteroidal antiinflammatory drugs. Endocrinology 150 (2), 1025–1032. https://doi.org/10.1210/en.2008-0188.
Wirth, E.K., Roth, S., Blechschmidt, C., Hölter, S.M., Becker, L., Racz, I., Zimmer, A., Klopstock, T., Gailus-Durner, V., Fuchs, H., Wurst, W., Naumann, T., Bräuer, A., de Angelis, M.H., Köhrle, J., Grüters, A., Schweizer, U., 2009. Neuronal 3′,3,5-triiodothyronine (T3) uptake and behavioral phenotype of mice deficient in Mct8, the neuronal T3 transporter mutated in Allan-Herndon-Dudley syndrome. J. Neurosci. 29 (30), 9439–9449. https://doi.org/10.1523/JNEUROSCI.6055-08.2009.
Xi, J., Su, X., Wang, Z., Ji, H., Chen, Y., Liu, X., Miao, M., Liang, H., Yuan, W., 2023. The associations between concentrations of gestational bisphenol analogues and thyroid related hormones in cord blood: a prospective cohort study. Ecotoxicol. Environ. Saf. 256 https://doi.org/10.1016/j.ecoenv.2023.114838.
Xiang, D., Han, J., Yao, T., Wang, Q., Zhou, B., Mohamed, A.D., Zhu, G., 2017. Structure-based investigation on the binding and activation of typical pesticides with thyroid receptor. Toxicol. Sci. 160 (2), 205–216. https://doi.org/10.1093/toxsci/kfx177.
Zoeller, T., Dowling, A., Herzig, C., Iannacone, E., Gauger, K., Bansal, R., 2002. Thyroid hormone, brain development, and the environment. Environ. Health Perspect. 110 (3), 335–361.
Zuang, V., Dura, A., Asturiol Bofill, D., Batista Leite, S., Berggren, E., Bernasconi, C., Bopp, S., Bowe, G., Campia, I., Carpi, D., Casati, S., Coecke, S., Cole, T., Corvi, R., Deceuninck, P., Fortaner Torrent, S., Franco, A., Gribaldo, L., Grignard, E., Whelan, M., 2020. EURL ECVAM status report on the development, validation and regulatory acceptance of alternative methods and approaches (2019). In: Publications Office of the European Union, Luxembourg. https://doi.org/10.2760/25602.